

# Magnetic and transport behaviors of non-centrosymmetric $\text{Nd}_7\text{Ni}_2\text{Pd}$

Cite as: AIP Advances **10**, 015103 (2020); <https://doi.org/10.1063/1.5129907>

Submitted: 02 October 2019 . Accepted: 21 November 2019 . Published Online: 02 January 2020

Arjun K. Pathak , Y. Mudryk , A. Provino, P. Manfrinetti, and V. K. Pecharsky



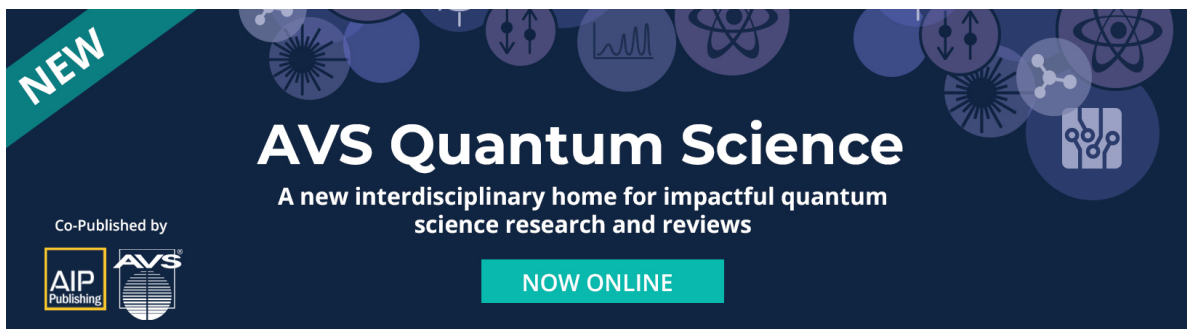
View Online



Export Citation



CrossMark





**NEW**

## AVS Quantum Science

A new interdisciplinary home for impactful quantum science research and reviews

Co-Published by



**NOW ONLINE**



# Magnetic and transport behaviors of non-centrosymmetric Nd<sub>7</sub>Ni<sub>2</sub>Pd

Cite as: AIP Advances 10, 015103 (2020); doi: 10.1063/1.5129907  
Presented: 5 November 2019 • Submitted: 2 October 2019 •  
Accepted: 21 November 2019 • Published Online: 2 January 2020



Arjun K. Pathak,<sup>1,a)</sup> Y. Mudryk,<sup>2</sup> A. Provino,<sup>3,4</sup> P. Manfrinetti,<sup>3,4</sup> and V. K. Pecharsky<sup>2,5</sup>

## AFFILIATIONS

<sup>1</sup>Department of Physics, SUNY Buffalo State, Buffalo, New York 14222, USA

<sup>2</sup>The Ames Laboratory, U.S. Department of Energy, Iowa State University, Ames, Iowa 50011, USA

<sup>3</sup>Department of Chemistry, University of Genova, 16146 Genova, Italy

<sup>4</sup>Institute SPIN-CNR, 16152 Genova, Italy

<sup>5</sup>Department of Materials Science and Engineering, Iowa State University, Ames, Iowa 50011, USA

**Note:** This paper was presented at the 64th Annual Conference on Magnetism and Magnetic Materials.

**Corresponding author:** pathakak@buffalostate.edu

## ABSTRACT

Crystallographic, magnetic, electrical transport and thermodynamic properties of pseudo-binary Nd<sub>7</sub>Ni<sub>2</sub>Pd compound have been studied using temperature-dependent x-ray powder diffraction and physical property measurements. Compared to the ferromagnetic parent Nd<sub>7</sub>Pd<sub>3</sub>, the ground state of Nd<sub>7</sub>Ni<sub>2</sub>Pd is antiferromagnetic, and it exhibits strong metamagnetism. The measurements indicate two antiferromagnetic transitions in fields less than 8 kOe: a second-order paramagnetic to antiferromagnetic at T<sub>N2</sub> = 29 K and a weak first-order antiferromagnetic to antiferromagnetic transition at T<sub>N1</sub> = 24.5 K. The compound becomes ferromagnetic in fields of 8 kOe and higher with T<sub>C</sub> = 30 K. Temperature dependence of lattice parameters is anomalous, most prominently in the basal plane at ~30 K; however, there is no detectable structural distortion or clear volume discontinuity around 25 K, suggesting a significant weakening of the first-order transition when compared to the binary Nd<sub>7</sub>Pd<sub>3</sub>.

© 2020 Author(s). All article content, except where otherwise noted, is licensed under a Creative Commons Attribution (CC BY) license (<http://creativecommons.org/licenses/by/4.0/>). <https://doi.org/10.1063/1.5129907>

## INTRODUCTION

Rare earth (R) intermetallic compounds are central to the condensed matter physics, solid-state chemistry, and materials science communities because of peculiar physical properties arising from the interplay between the localized and delocalized electronic states, which can be manipulated by tailoring their chemical and crystallographic makeups.<sup>1–5</sup> Among a broader class of rare-earth-based materials, compounds lacking the center of inversion are rather rare but they often exhibit physical behaviors of both fundamental and practical significance.<sup>6–8</sup> In particular, R<sub>7</sub>Pd<sub>3</sub> compounds with R = La-Nd, Sm, Gd crystallize in the hexagonal Th<sub>7</sub>Fe<sub>3</sub> structure type described by the non-centrosymmetric space group symmetry *P6<sub>3</sub>mc*. In this type of crystal structure, the Pd atoms reside on a single 6*c* site, while the R atoms occupy three different crystallographic sites (2×6*c* and 2*b*), resulting in three different magnetic sub-lattices formed by the lanthanide atoms.<sup>9–11</sup>

The magnetic and electrical properties of Nd<sub>7</sub>Pd<sub>3</sub><sup>12–15</sup> show that upon cooling the compound undergoes at least two phase transitions: a second-order paramagnetic (PM) – antiferromagnetic (AFM) ordering at T<sub>N</sub> ~ 37 K, which is followed by an hysteretic first-order phase transition from the AFM to a ferromagnetic (FM) state at T<sub>C</sub> ~ 33 K. Recently it was demonstrated that the first-order transition at T<sub>C</sub> is a symmetry-driven magneto-structural transformation between the high-temperature hexagonal and the low-temperature orthorhombic (space group *Cmc2<sub>1</sub>*) crystal structures.<sup>16</sup> The structural distortion in Nd<sub>7</sub>Pd<sub>3</sub> occurs because the non-centrosymmetric *P6<sub>3</sub>mc* adopted by both PM and AFM parents does not support a stable FM state; on the other hand, *Cmc2<sub>1</sub>*, which is a subgroup of *P6<sub>3</sub>mc*, makes a collinear arrangement of the three independent Nd sublattices in the FM state possible. It is worth noting, however, that even though the first-order character of the AFM-FM transition in Nd<sub>7</sub>Pd<sub>3</sub> is clearly established, the distortion itself is subtle: it could not be detected with laboratory x-ray diffraction

or with high-resolution neutron diffraction and was only observed using high-resolution synchrotron data.<sup>16</sup>

Even though physical properties of  $R_7Pd_3$  with different  $R$  have been studied in the past,<sup>9,11,12</sup> the influence of partial substitution of the  $4d$  Pd with a  $3d$  element on the magnetism and transport has been not, leaving a wealth of potentially interesting magnetism unexplored. Since the  $3d$  electrons of, e.g. Ni, are less localized, than  $4d$  electrons of Pd<sup>17</sup> and, especially, than  $4f$  electrons of Nd, one may expect varying competition of localized and itinerant magnetism, and even more complex magnetic structures in  $Nd_7Ni_xPd_{3-x}$  than in the binary  $Nd_7Pd_3$ . With this in mind, we report crystallographic, magnetic, transport, and calorimetric investigation of pseudo-binary  $Nd_7Ni_2Pd$  compound, where 2/3 of Pd atoms are randomly substituted by chemically similar Ni atoms.

## EXPERIMENTAL TECHNIQUES

Polycrystalline  $Nd_7Ni_2Pd$  was prepared by arc melting stoichiometric amounts of the constituent elements in an argon atmosphere, followed by annealing at 750 °C for one week and slow cooling to room temperature. Room-temperature crystal structure and phase purity were determined using x-ray powder diffraction (XRPD) using a PANalytical X'Pert diffractometer. XRPD measurements as a function of temperature at  $H = 0$  and 20kOe were carried out on a Rigaku TTRAX rotating anode powder diffractometer as described in Ref. 18. Both ac and dc magnetization measurements were performed in a superconducting quantum interference device magnetometer (Quantum Design) and a physical property measurement system (PPMS, Quantum Design). Heat capacity

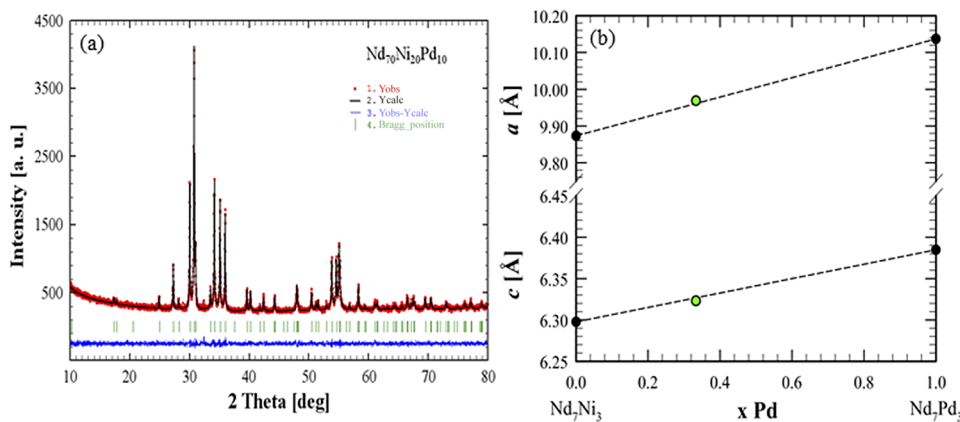


**FIG. 1.** (a) Observed and calculated XRPD patterns of  $Nd_7Ni_2Pd$  at  $T=300K$ . (b) The lattice parameters ( $a$  and  $c$ ) of  $Nd_7Ni_2Pd$ ,  $Nd_7Ni_3$ ,<sup>21</sup> and  $Nd_7Pd_3$ .<sup>16</sup>

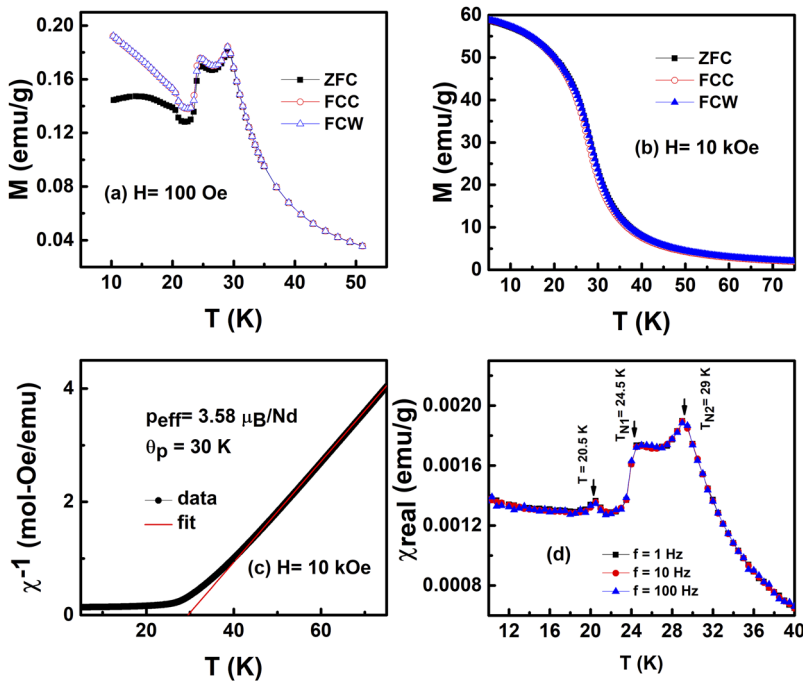


**FIG. 2.** ZFC, FCC, and FCW magnetization of  $Nd_7Ni_2Pd$  measured in (a)  $H = 100$  Oe, (b)  $H = 10kOe$ . (c) Inverse dc magnetic susceptibility  $\chi^{-1}(T)$  in  $H = 10kOe$  together with the Curie-Weiss fit of the data above 50K. (d) Temperature dependence of real part of ac magnetic susceptibility measured in ac driving field with 1 Oe amplitude and frequencies from 1 to 100 Hz.

( $C_p(T)$ ) and ac electrical transport measurements were performed using PPMS.

## RESULTS AND DISCUSSION

The XRPD data at  $T = 300\text{K}$  show that  $\text{Nd}_7\text{Ni}_2\text{Pd}$  is practically single phase with hexagonal  $\text{Th}_7\text{Fe}_3$ -type structure ( $hP20$ ,  $P6_3mc$ , No. 186). The only Bragg reflection not matching the  $\text{Nd}_7\text{Ni}_2\text{Pd}$  phase corresponds to a very weak peak at  $2\theta = 32.4^\circ$  (Fig. 1a), which may be attributed to a trace amount of  $\text{NdNi}_{1-x}\text{Pd}_x$ . The obtained values of lattice parameters are  $a = 9.9716(2)\text{ \AA}$ , and  $c = 6.3231(2)\text{ \AA}$ , lower than those of the  $\text{Nd}_7\text{Pd}_3$ . They, as well as the unit cell volume, lie on straight lines connecting the corresponding values of

$\text{Nd}_7\text{Pd}_3$  and  $\text{Nd}_7\text{Ni}_3$ , as expected for a Ni/Pd composition ratio of 2/1 (Fig. 1b).

The zero-field cooled (ZFC), field-cooled cooling (FCC), and field-cooled warming (FCW) magnetization  $M(T)$  data measured at  $H = 0.01$ , and  $10\text{ kOe}$  are shown in Fig. 2. The substitution of Ni for Pd in  $\text{Nd}_7\text{Pd}_3$  leads to an AFM ground state with AFM transitions at  $T_{\text{N}1} = 24.5\text{K}$  and  $T_{\text{N}2} = 29\text{K}$ . The transition at  $T_{\text{N}1}$  (see  $C_p(T)$  below) is likely weakly first-order transformation. With increasing magnetic field,  $M(T)$  anomaly at  $T_{\text{N}1}$  becomes more pronounced than the one at  $T_{\text{N}2}$ , and both peaks disappear at  $H \geq 10\text{ kOe}$  when the compound becomes FM (Fig. 2b). The Curie temperature,  $T_{\text{C}}$ , obtained from  $M(T)$  data at  $H = 10\text{ kOe}$  and defined as the minimum value of  $dM/dT$ , is  $30\text{K}$ . The inverse dc magnetic susceptibility

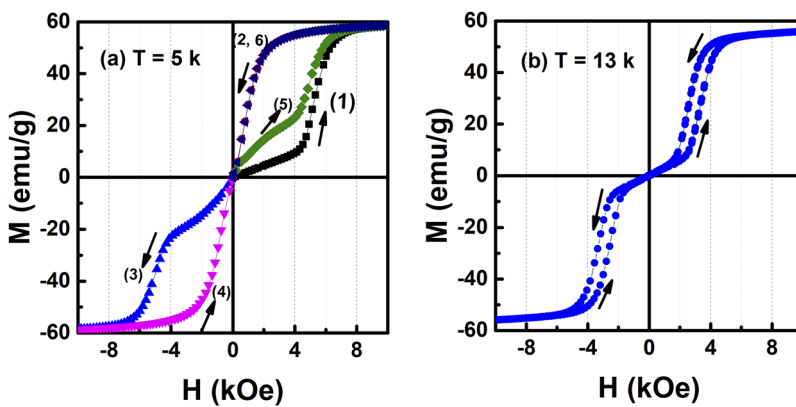


**FIG. 3.**  $M(H)$  measured at (a)  $T = 5\text{ K}$  and (b)  $T = 13\text{ K}$ . The magnetization was measured up to  $\pm 90\text{ kOe}$  but only the low field data are shown for clarity. The hysteresis loops were recorded after cooling the sample in a zero magnetic field followed by changing the magnetic field from  $0$  to  $90\text{ kOe}$  (1<sup>st</sup> cycle), then  $90 \rightarrow -90\text{ kOe}$  (2<sup>nd</sup>, and 3<sup>rd</sup> cycle), then  $-90 \rightarrow +90\text{ kOe}$  (4<sup>th</sup>, and 5<sup>th</sup> cycle), and finally  $+90 \rightarrow 0\text{ kOe}$  (6<sup>th</sup> cycle).

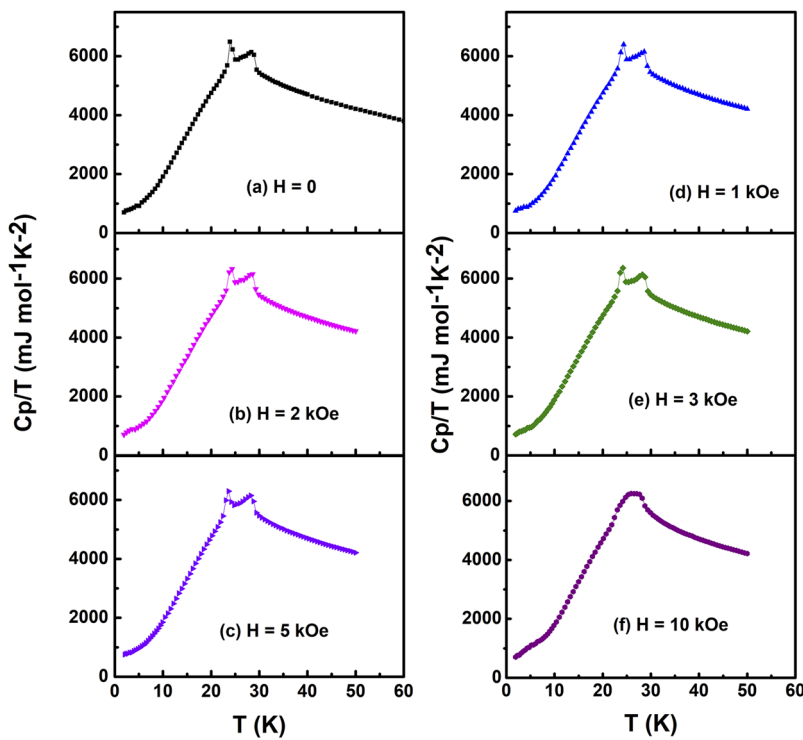


**FIG. 4.** (a-f) Heat capacity  $C_p$  of  $\text{Nd}_7\text{Ni}_2\text{Ni}$  measured in magnetic fields up to  $10\text{ kOe}$ .

( $\chi^{-1} = H/M$ ) follows the Curie-Weiss law. The effective magnetic moments,  $p_{\text{eff}}$ , and Weiss temperature,  $\theta_p$ , are  $3.58 \mu_B/\text{Nd}$  and 30 K, respectively. The former is in a very good agreement with the  $g[J(J+1)]^{1/2} = 3.62 \mu_B$  value of  $\text{Nd}^{3+}$  while the positive  $\theta_p$  value that is identical to  $T_C$  points to the dominance of FM interactions in the compound. Ac magnetic susceptibility measured in an ac field of 1 Oe with zero bias dc magnetic field at different frequencies shown in Fig. 2d. Consistent with  $M(T)$ , a real part of ac susceptibility shows two AFM transitions  $T_{N1} = 24.5$  K and  $T_{N2} = 29$  K and an additional peak at 20.5 K, which is different from that observed in  $\text{Nd}_7\text{Pd}_3$ , where it occurs at 16 K and is due to the NdPd impurity.<sup>19</sup> Fillion *et al.*<sup>20</sup> reported that NdNi orders FM at 28K, suggesting the peak at 20.5K observed in  $\text{Nd}_7\text{Ni}_2\text{Pd}$  is due to a pseudo-binary  $\text{NdNi}_{1-x}\text{Pd}_x$  phase, also detected in the XRPD data.

$M(H)$ , at  $T = 5$  and 13 K measured on a ZFC sample is shown in Fig. 3. Consistent with low-field  $M(T)$  data, ZFC  $M(H)$  clearly shows the AFM ground state both at  $T = 5$  and 13 K. When the magnetic field increases,  $M(H)$  at 5 K indicates a robust meta-magnetic behavior with a critical field  $\sim \pm 4$  kOe, and the compound becomes FM with magnetization approaching saturation when  $H$  reaches and exceeds  $\pm 8$  kOe. The metamagnetic behavior is also observed at 13 K (Fig. 3b) and the critical field decreases to about  $\pm 3$  kOe. The saturation magnetization is  $2.03 \mu_B/\text{Nd}^{3+}$ , which is slightly higher compared to that of  $\text{Nd}_7\text{Pd}_3$  ( $1.8 \mu_B/\text{Nd}^{3+}$ ).<sup>12,16</sup>

Heat capacity,  $C_p(T)$ , measured at various external magnetic fields (illustrated as  $C_p/T$  in Fig. 4) clearly shows two peaks corresponding to  $T_{N1}$  and  $T_{N2}$  observed in  $M(T)$  data. The relatively sharp and rather narrow peak at  $T_{N1}$  suggests a first-order phase transition at  $T_{N1}$ . Both peaks at  $T_{N1}$  and  $T_{N2}$  remain practically unchanged up to 5 kOe, but the two anomalies merge into a single broad maximum when the applied field is  $H = 10$  kOe, which is typical for second-order phase transitions. The absence of  $C_p/T$  anomaly at  $T = 16$  K confirms that the corresponding peak seen in the ac magnetic susceptibility data of Fig. 2d is likely from a minor impurity.

The electrical resistivity,  $\rho(T)$ , is nearly temperature independent at  $T \leq 7$  K (Fig. 5), increasing afterward, indicating metallic behavior. The anomaly is observed near  $T_{N1} = 29$  K and a minor

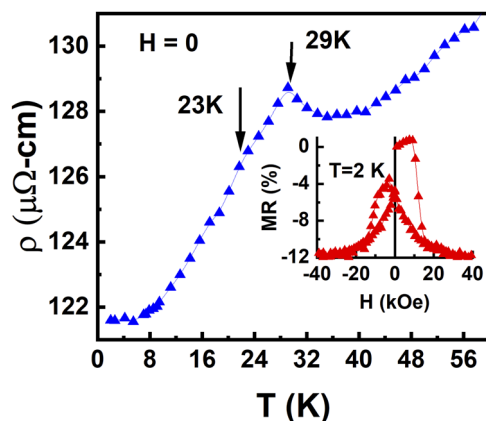


FIG. 5. Electrical resistivity of  $\text{Nd}_7\text{Ni}_2\text{Pd}$  measured as a function of temperature at zero magnetic field. Inset shows magnetoresistance measured as a function of magnetic field at  $T=2$  K.

peak is observed at  $T_{N2} = 23$  K.  $\rho(H)$  shows a sharp change when the sample transforms from the AFM to FM state and it saturates when the compound is firmly in the FM state for  $H \geq 10$  kOe. The magnetoresistance (Fig. 5, inset) reaches  $-12\%$ . Incomplete reversibility of magnetoresistance is related to similar irreversibilities seen in  $M(H)$  data at 5 K, Fig. 3a.

The temperature dependent XRPD at  $H = 0$  and 20 kOe show that the compound crystallizes in the  $\text{Th}_7\text{Fe}_3$  structure type in the whole temperature region. However, considering that the structural distortion was not observed with laboratory XRPD in  $\text{Nd}_7\text{Pd}_3$ <sup>16</sup> we cannot rule out that a similar weak  $P6_3mc \rightarrow Cmc2_1$  distortion also occurs in  $\text{Nd}_7\text{Ni}_2\text{Pd}$ . If fact, given that FM state is not supported by the hexagonal  $P6_3mc$ , it is nearly certain that the structural distortion is indeed present in  $\text{Nd}_7\text{Ni}_2\text{Pd}$ ; high-resolution synchrotron XRPD

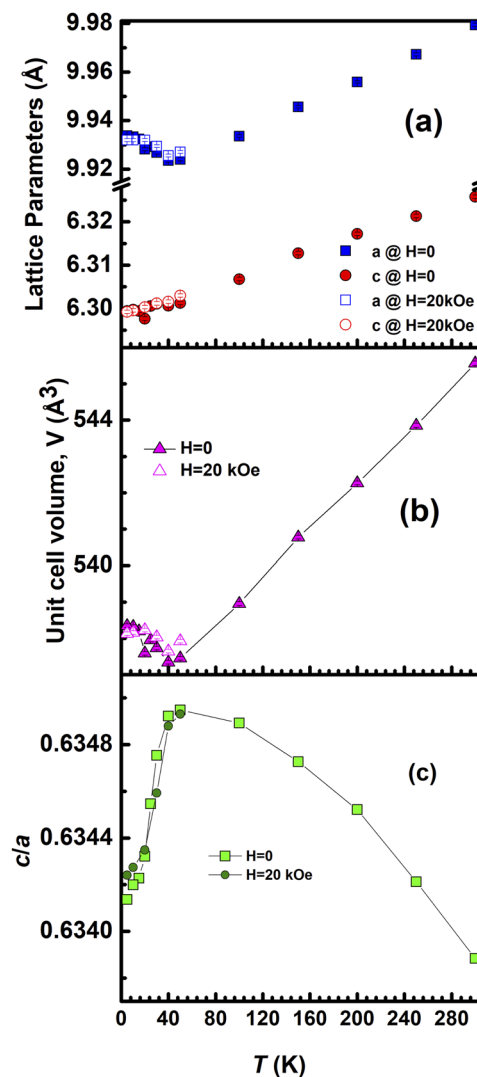


FIG. 6. Temperature dependencies of lattice parameters (a), unit cell volume (b) and  $c/a$  ratio (c) of  $\text{Nd}_7\text{Ni}_2\text{Pd}$  determined from Rietveld refinement of XRPD data.

measurements are likely required to demonstrate this symmetry altering transition. At the same time, partial substitution of Pd with Ni in Nd<sub>7</sub>Ni<sub>2</sub>Pd practically removes the discontinuous behavior of lattice parameters, both at 0 and 20 kOe (Fig. 6), which explains the very weak first-order character of the low-temperature transition. However, the contraction along c axis as well as the expansion along the a-axis, and the resulting decrease of the c/a ratio and the increase of the unit cell volume in the magnetically ordered state are observed in both the parent Nd<sub>7</sub>Pd<sub>3</sub> and in the Ni substituted Nd<sub>7</sub>Ni<sub>2</sub>Pd. The application of the magnetic field has a negligible effect on the lattice parameters.

## SUMMARY

We show that partial substitution of Pd with Ni changes the ground state from FM in Nd<sub>7</sub>Pd<sub>3</sub> to AFM in Nd<sub>7</sub>Ni<sub>2</sub>Pd. The AFM transition that occurs upon cooling at T<sub>N1</sub> = 24.5 K is weakly first order, and it is preceded by a second-order AFM ordering at T<sub>N2</sub> = 29 K. The ρ(T,H) show metallic behavior with magnetoresistance reaching -12% at H = 30 kOe and T = 2 K. Temperature-dependent XRPD reveals anomaly in the lattice parameter *a* at ~30 K, however, there is no detectable structural distortion or volume discontinuity around 25 K, suggesting a significant weakening of the first-order transition compared to the binary Nd<sub>7</sub>Pd<sub>3</sub>. Compared to Nd<sub>7</sub>Pd<sub>3</sub>, Nd<sub>7</sub>Ni<sub>2</sub>Pd exhibits strong metamagnetic behavior with the application of an external magnetic field.

## ACKNOWLEDGMENTS

The Ames Laboratory is operated for the U. S. Department of Energy by Iowa State University of Science and Technology under contract No. DE-AC02-07CH11358. This work was supported by the Department of Energy, Office of Basic Energy Sciences, Materials Sciences Division. AKP acknowledges the start-up funding from SUNY Buffalo State to present this work. AP and PM acknowledge the Institute SPIN of the CNR, the Department of Chemistry of the University of Genova and the NEWS project (No. 734303) to support their stay at the Ames Laboratory.

## REFERENCES

- <sup>1</sup>S. Xu, F. Jia, Y. Yang, L. Qiao, S. Hu, D. J. Singh, and W. Ren, *Phys. Rev. B* **100**, 104408 (2019).
- <sup>2</sup>C. Shekhar, N. Kumar, V. Grinenko, S. Singh, R. Sarkar, H. Luetkens, S. Wu, Y. Zhang, A. C. Komarek, E. Kampert, Y. Skourski, J. Wosnitza, W. Schnelle, A. McCollam, U. Zeitler, J. Kübler, B. Yan, H.-H. Klauss, S. S. P. Parkin, and C. Felser, *PNAS* **115**, 9140 (2018).
- <sup>3</sup>E. Gratz, *J. Mag. Mag. Mater.* **254**, 1 (1981).
- <sup>4</sup>A. Kowalczyk, T. Tolinski, B. Andrzejewski, and A. Szlaferek, *J. Alloys Compd.* **413**, 1 (2006).
- <sup>5</sup>A. V. Morozkin, R. Nirmala, J. Yao, Y. Mozharivskiy, and O. Isnard, *J. Solid State Chem.* **196**, 93 (2012).
- <sup>6</sup>P. Shiv Halasyamani and K. R. Poeppelmeier, *Chem. Mater.* **10**, 2753 (1998).
- <sup>7</sup>A. N. Bogdanov, U. K. Rößler, M. Wolf, and K.-H. Müller, *Phys. Rev. B* **66**, 214410 (2002).
- <sup>8</sup>Y. Tokunaga, X. Z. Yu, J. S. White, H. M. Rønnow, D. Morikawa, Y. Taguchi, and Y. Tokura, *Nat. Comms.* **6**, 7638 (2015).
- <sup>9</sup>J. M. Moreau and E. Parthé, *J. Less-Comm. Met.* **32**, 91 (1973).
- <sup>10</sup>J. V. Florio, N. C. Baenziger, and R. E. Rundle, *Acta Cryst.* **9**, 367 (1956).
- <sup>11</sup>H. Kadomatsu, K. Kuwano, K. Umeo, Y. Itoh, and T. Tokunaga, *J. of Mag. and Mag. Mat.* **189**, 335 (1998).
- <sup>12</sup>N. K. Singh, P. Kumar, Z. Mao, D. Paudyal, V. Neu, K. G. Suresh, V. K. Pecharsky, and K. A. Gschneidner, Jr., *J. Phys.: Condens. Matter* **21**, 456004 (2009).
- <sup>13</sup>T. Matsushita, K. Shimomura, and T. Tsutaoka, *J. Korean Physical Society* **63**, 559 (2013).
- <sup>14</sup>P. Kumar, P. Jaina, and R. Kumar, *RSC Advances* **5**, 58928 (2015).
- <sup>15</sup>F. Canepa, M. Napolitano, and S. Cirafici, *Intermetallics* **10**, 731 (2002).
- <sup>16</sup>Y. Mudryk, C. Ritter, D. Paudyal, A. Provino, S. K. Dhar, P. Manfrinetti, and V. K. Pecharsky, *J. Phys.: Condens. Matter* **31**, 265801 (2019).
- <sup>17</sup>B. R. Coles and D. Phil, *Platinum Metal Rev* **8**(1), 9 (1964).
- <sup>18</sup>A. P. Holm, V. K. Pecharsky, K. A. Gschneidner, R. Rink, and M. N. Jirmanus, *Rev. Sci. Instrum.* **754**, 1081 (2004).
- <sup>19</sup>V. Dhar and A. Provino, *Solid State Comms* **242**, 46 (2016).
- <sup>20</sup>G. Fillion, D. Gignoux, F. Givord, and R. Lemaire, *J. Magn. Magn. Mat.* **44**, 173 (1984).
- <sup>21</sup>T. Tsutaoka, Y. Andoh, S. Kawano, G. Nakamoto, D. T. Kim Anh, M. Kurisu, and T. Tokunaga, *J. Alloys Compd.* **408**, 181 (2006).